This is a pre print version of the following article:

On the chemical condensation of the layers of zeolite precursor MCM-22(P) / Fabbiani, M., Morsli, A., Confalonieri, G., Cacciaguerra, T., Fajula, F., Haines, J., Bengueddach, A., Arletti, R., Di Renzo, F.. - In: MICROPOROUS AND MESOPOROUS MATERIALS. - ISSN 1387-1811. - 332:(2022), pp. 111678-111678. [10.1016/j.micromeso.2021.111678]

Terms of use:

The terms and conditions for the reuse of this version of the manuscript are specified in the publishing policy. For all terms of use and more information see the publisher's website.

03/06/2026 00:44

(Article begins on next page)

On the chemical condensation of the layers of zeolite precursor MCM-22(P)

Marco Fabbiani[a], Amine Morsli[b], Giorgia Confalonieri[c], Thomas Cacciaguerra[a], François Fajula[a], Julien Haines[a], Abdelkader Bengueddach[d], Rossella Arletti[e], Francesco Di Renzo[a,*]

[a] *ICGM, Univ Montpellier-CNRS-ENSCM, Centre Balard, 1919 route de Mende, 34090 Montpellier, France, *francesco.di-renzo@umontpellier.fr*

[b] *LIPE, Laboratory of Engineering of Environmental Processes, University of Science and Technologies of Oran "M. Boudiaf", BP 1505, Oran El M'Nouer, Algeria, morsli_amine@yahoo.fr*

[c] *ESRF, 71 Av. des Martyrs, 38000 Grenoble, France, giorgia.confalonieri@esrf.fr*

[d] *Laboratory of Chemistry of Materials, Faculty of Applied and Exact Sciences, University of Oran, BP 1524, Oran, Algeria, abengueddach@gmail.com*

[e] *Department of Chemical and Geological Sciences, University of Modena and Reggio Emilia, Via Giuseppe Campi 103, 41125 Modena, Italy, rossella.arletti@unimore.it*

Abstract

Chemical condensation of layers of silicates has been often proposed as an alternative to thermal condensation, finding limited success. The formation of the industrially relevant MCM-22 zeolite (MWW IZA code) from a mild hydrothermal precursor is the most important example of 2D-3D aluminosilicate condensation. Silanols of opposed layers have been condensed by acid-driven dehydration in concentrated nitric acid, as

confirmed by powder XRD and ^{29}Si NMR spectroscopy, implying interlayer template extraction and corresponding dealumination. Milder acid treatments favour template extraction and shrinkage of interlayer distance, but do not provide significant silanol condensation. Template extraction is further favoured by degradation of the organics in the presence of a Cu^{2+} homogeneous catalyst.

Keywords: zeolite, layered material, acid condensation, template extraction, dealumination

1. Introduction

Layered zeolite precursors present a two-pronged interest: (a) their layers can be separated without breaking any siloxane bond to form delaminated materials, which feature zeolitic active sites but provide faster access to bulkier substrates [1]; (b) in some cases, the use of appropriate templates can orient their condensation towards different 3D zeolite structures [2-4].

Several examples of formation of 3D (3-dimensional) zeolites from 2D (2-dimensional) layered precursors have been reported and extensively reviewed [5-9]. After the pioneering work of the groups of Lowe [10] and Guth [11] groups on the precursors of, respectively, Eu-20 and ferrierite, it was shown that several zeolites can be formed from 2D intermediates, like Nu-6 [12], CDS-1 [13], RUB-24 [14], RUB-41 [15], sodalite [16], MCM-35 [17]. 2D layered materials have not only been formed by classical hydrothermal methods, but have also been prepared by selective chemical delamination of 3D zeolites [18-21]. These 2D materials have been assembled to form different 3D

structures, in the ADOR (assembly-disassembly-organisation-reassembly) zeolite synthesis method [22]. Among all these 2D precursors, MCM-22(P), the layered precursor of MCM-22 (IZA structure code MWW), has represented the main instance of development of useful materials from 2D zeolite layers [6, 23].

MCM-22 itself has entered the industrial market as a major catalyst in benzene alkylation processes [24-26]. The understanding of the layered structure of the precursor was a step-by-step process. Also before the determination of the P6/mmm MCM-22 structure [27], it was reported that several materials with MWW structure were formed by calcination of a common precursor, issued from hydrothermal synthesis at moderate temperature and featuring a distinct XRD pattern [28, 29]. The precursor (later usually called MCM-22(P)) evolved to the MCM-22 structure when calcined at temperature normally between 460 and 550 °C [28-30]. A layered structure for the MCM-22 precursor was early suggested by its easy swelling by surfactants to form MCM-36 pillared materials [31]. The XRD patterns of zeolite and precursor feature a striking characteristic: they present the same hk0 reflections, and only differ by the spacing and stacking of hk0 layers. The knowledge we have of the structure of the 2D precursor stems from this commonality of structure with the layers of the 3D zeolite. The layered structure of the precursor was described early on Millini et al. [32]. However, no proper structure refinement of MCM-22(P) has been published.

The layer common to the precursor and zeolite presents a sandwich-like cage structure, with a complex scaffold of aluminosilicate tetrahedra around SDA molecules. Along the c-axis, the scaffold presents a succession of 4-, 5-, and 6-member rings with as many as 12 tetrahedra between the opposite sides of the layer (Figure 1). At a local scale, the 2D

layer is indeed a 3D scaffold, with a much higher stability than most layered silicates, which present thinner layers [33].

The structure of MCM-22 presents an ordered alternation of two parallel non-interconnected 2D 10MR (rings formed by 10 tetrahedra) channel systems, defined as intralayer and interlayer pore systems. The intralayer one, with 5.5x4.0 Å sinusoidal channels, is already present in the layered precursor. The interlayer one, with 5.1x4.1 Å windows connecting large 18.2x7.1 Å supercages, is formed by the condensation of the precursor layers. The condensation of the 2D layered precursor to the 3D zeolite upon calcination of the template (SDA, structure-directing agent) implies a decrease of the *c* cell parameter, typically from 26.7 to 25.1 Å. This shrinkage brings about a shift of the XRD peaks with Miller index $l \neq 0$ and the 002 reflection moves to a higher angle and is virtually superposed to the 100 reflection (Figure 2). This change of the appearance of the XRD pattern has been generally considered as an indicator of condensation of the MCM-22(P) layers. However, it was shown that complete calcination of the sample was not needed to attain similar shrinkages of the *c* parameter, which can occur already at 250°C, with the elimination of just a fraction of the SDA [32].

Several SDAs allowed to form zeolites with an XRD pattern corresponding to the MWW network, well before the structure was resolved in 1994 [27]: hexamethylene imine (HMI) was used to form PSH-3 at Bayer in 1984 [36] and MCM-22 at Mobil in 1990 [37]; other heterocyclic amines were also used to form MCM-22 [38], HMI or piperidine was used to form borosilicate ERB-1 at ENI in 2008 [28]; quaternary adamantammonium allowed to form high-silica SSZ-25 at Chevron in 1989 [29] and all-silica ITQ-1 in 1996 [39]. Also the amount of SDA can play a significant role in the synthesis. Starving the synthesis system of organics, the SDA was preferentially

confined inside the intralayer pore system, the interlayer distance was shrunk and layers were directly condensed in mild hydrothermal conditions in the direct synthesis of MCM-49, a mildly disordered MWW material [38, 40, 41].

Several MWW-related materials have been formed, characterized by more or less disordered stacking of the layers. The properties of these materials have been extensively reported and reviewed [9, 42-44] The easy separation of the layers of the precursor by cation exchange of the SDA by surfactants (delamination) has opened access to the large characteristic cavities in the 2D sheets, providing easy accessibility to catalytic sites in the ITQ-2 material [1].

The porosity of as-synthesized zeolites is usually liberated by thermal degradation of SDA and emission of its degradation products. Methods to extract and recover the SDA have been attempted and found limited success, essentially for 12MR large-pore zeolites [45, 46]. In the case of aluminosilicate zeolites with 12MR pores, thermal treatments could be replaced by severe nitric acid leaching, accompanied by extended dealumination [47]. This kind of treatment has been shown to simultaneously extract SDA and incorporate transition metal cations in a zeolite network [48, 49]. The results of relatively milder treatments by acetic acid were strongly dependent on the relative size of SDA and zeolite windows, as well as on the composition of the zeolite, which affected the strength of the interaction between SDA and network sites [50]. In the case of the 12MR BEA zeolite, effective extraction of tetraethylammonium (TEA) SDA was reached for the all-silica zeolite but was less effective for the borosilicate form and much less effective for the aluminosilicate form, presenting stronger Brønsted acid sites. For the 10MR MFI zeolite, extraction was possible only if the composition was all-silica and a linear SDA was used.

The piperidine SDA of the precursor of MWW borosilicate ERB-1 was easily extracted from the interlayer space by a very mild treatment with acetate solution [32]. A corresponding 1 Å shrinkage of the *c* cell parameter was observed. In the case of aluminosilicate MCM-22(P), the results of a treatment with 2 M HNO_3 were highly dependent on the nature of the SDA [51]. In the case of piperidine-templated MCM-22(P), the acid treatment brought to complete superposition of 002 and 100 reflections, which was interpreted as a condensation of the layers into MCM-56, a material with partially disordered MWW structure. However, in the presence of the slightly larger HMI SDA, the acid treatment did not bring any modification of the XRD pattern of MCM-22(P).

Effective extraction of HMI SDA from the MWW precursor was reported by dielectric-barrier discharge (DBD) plasma treatments at temperature not expected to exceed 125 °C [52]. Complete extraction of the SDA brought to a modification of the XRD pattern compatible with a condensation of the layers of MCM-22(P) to the MCM-22 structure.

The interest for the conditions of 2D to 3D condensation of silicates have received increased attention since the realisation that several networks can be formed by orienting the establishment of interlayer bonds by appropriate amount or nature of organics [53-55]. The development of methods for silanol condensation alternative to thermal treatment is receiving increasing attention [56, 57]. The purpose of this work is to analyse at which point the extraction by chemical tr6eatment of a fraction of SDA can vicariate thermal treatment in the condensation of tridimensional networks from bidimensional precursors. The condensation of MCM-22(P) to MWW network appears to be an ideal case study.

2. Experimental

The precursor MWW(P) was prepared by adding hexamethyleneimine (HMI) and Aerosil 200V fumed silica to an alkaline aqueous solution of sodium aluminate, forming a gel of molar composition Na 0.133 / HMI 0.500 / Al 0.030 / Si / H_2O 45. The gel was sealed in a stainless steel autoclave, heated at 150 °C under stirring at 60 rpm for 7 days, cooled down, filtered and water-washed.

The HMI-templated aluminosilicate layered precursor MWW(P) has been subjected to several treatments aimed at the low-temperature extraction of the SDA.

1) Treatment by diluted acid in mixed solvent: MWW(P) was stirred in a 20% w/w 1,4-dioxane aqueous solution with pH controlled by HCl addition. The solid/liquid ratio was 10 g/L. After 4 h stirring at 30 °C, the solid was filtered, water-washed and dried at 80°C. The samples are called pH#, where # is the pH of the treatment.

2) Treatment by diluted acid in mixed solvent in the presence of Cu^{2+}: as in previous treatment with addition of $CuCl_2$ in the solution. The samples are called CupH#E&, where # is the pH of the treatment and E& the molar Cu^{2+} concentration expressed as powers of ten. For instance, CupH4E-2 is sample MWW(P) treated by a 0.02 M $CuCl_2$ and 20% w/w 1,4-dioxane aqueous solution brought to pH4.

3) Treatment by concentrated acid: MWW(P) was refluxed in 70% HNO_3 10 h with a solid/liquid ratio 10 g/L, cooled down, filtered, washed with 4 M HNO_3, water-washed and dried at 80 °C. The treated sample is called AA.

The solids formed, as prepared and calcined at 550°C in air flow (calcined samples are indicated by a letter C after their name), were characterized by elemental analysis (CNRS Service Central d'Analyse, Solaize), thermal gravimetry (Setaram TG 85

microbalance in air flow), powder X-ray diffraction (Bruker AXS D8 diffractometer, Θ-Θ setting, Cu Ka radiation, Ni filter), Scanning electron microscopy (SEM) (Hitachi S-4500 microscope), FT-IR (KBr wafers, Nicolet 320 spectrometer) and hpdec ^{29}Si MAS-NMR spectroscopy (Bruker ASX 400 spectrometer, 79.5 MHz).

The deconvolution of the complex MWW ^{29}Si MAS-NMR signals was performed by the procedure originally suggested by Weitkamp and coworkers [58]. The initial point for the deconvolution was provided by the Si(0Al) T2 peak at nearly -120 ppm, which indicated the area of the Si6 peak, corresponding to 12 tetrahedra p.u.c (per unit cell). Peaks of other tetrahedron sites were located at chemical shifts corresponding to the Si-O-Si angles of ITQ-1, the all-silica MWW, attributing them areas proportional to the mutiplicity of each site: 12 tetrahedra p.u.c. for the *m* sites and 4 tetrahedra p.u.c. for the *3m* sites [39, 59-61]. Si(1Al) peaks were located 6 ppm upfield the corresponding Si(0Al) signals, with initial area proportional to the amount of Al in the sample according to the Engelhardt correlation [62]. A simplifying assumption of equivalent fraction of Al in the eigth crystallographic sites was used. When needed, Q3 Si(1OH) peaks were located nearly 10 ppm upfield from the corresponding Si(0Al) signals [63].

3. Results and discussion

3.1. Diluted acid treatments

Dehydration-condensation of the silanols of layered silicates by 10 M acetic acid was proposed by Oumi et al. [64]. In the case of the ERB-1 precursor, leaching by acetate solutions was effective in the extraction of piperidine, leading to a significant decrease of the *c* cell parameter [32]. However, in this case, the decrease of interlayer space did

not correspond to a condensation of the layers, as it was reversible and the *c* parameter was increased again by intercalation of organic solvents. When nitric acid was used, a partial dealumination of MCM-22(P) was observed, less than 10% aluminium being extracted by 6 M HNO_3 at 100 °C [65]. Partial extraction of the SDA could be achieved in milder conditions. Treatments by 2 M HNO_3 at room temperature were able to decrease the *c* cell parameter, leading to a diffraction pattern corresponding to a disordered MCM-56 [51]. However, the effectiveness of the treatment was highly dependent on the nature of the SDA, interlayer shrinkage being observed in the case of piperidine-templated MCM-22(P), but not for the material templated by the slightly larger HMI. We attempted to couple solvent extraction and acid leaching by using more diluted nitric acid in the presence of an organic solvent, intendended to facilitate the extraction of HMI.

Composition and crystallographic data of the as-synthesized and acid-treated samples are reported in Table 1. Precursor sample MWW(P) featured a Si/Al ratio 23 and an organic content corresponding to nearly 10 HMI molecules per unit cell, in good agreement with the location of the SDA in the intralayer sinusoidal channels as well as in the interlayer region [40]. Calcination of MWW(P) at 550°C completely removed the SDA and modified the XRD pattern from a typical MCM-22(P) to a MWW pattern (Figure 3). The MWW(P)C crystals presented a well-defined lamellar morphology, with a thickness along the c axis corresponding to about 10 cell parameters (Figure 4). The effects of treatments at room temperature by 20% dioxane nitric acid aqueous solution were highly dependent on the pH level. Treatments at pH 4 and 3 led to a slight narrowing of the diffraction peaks, accompanied by limited extraction of organics and decrease of the c parameter from pH 3. Treatment at pH 2 brought to a broadening of

the diffraction lines with $l \neq 0$ and to a decrease of the *c* value to 25.7 Å. Treatment at pH 1 caused the extraction of nearly 43 % SDA and a decrease of the c parameter to 25 Å, a value comparable to the effect of calcination at 550°C. The sample pH1 presented two broad peaks centered at 8.5 and 9.7 °2Θ, probably corresponding to 101 and 102 peaks shifted by interstratification effect [66-68]. Such a diffraction pattern corresponds to literature reports on MCM-49, the–MWW material formed by synthesis with low SDA and high Na content [38, 40]. No more than 5% aluminium of the sample was removed by the treatment, also at pH 1.

In all samples, the retention of the layer structure was witnessed by the stability of the hk0 reflections, unaffected by the decrease of the *c* cell parameter. The c value reached in the sample pH1 with the loss of nearly half of the organic template corresponded to a selective extraction of HMI from the interlayer space. The broadening of the XRD peaks with $l \neq 0$ suggests a decrease of the coherent domain in the *c* direction, corresponding to a significant stacking disorder. A mismatch between layers could account for the decrease of the *c* parameter in sample pH1 to a value lower than in the calcined MWW(P)C sample. In all cases, the lamellar morphology of the crystals (Figure 4), unchanged by leaching or calcination treatment, showed a length along the *c* axis not larger than 10 unit cells.

MWW-type materials present characteristic ^{29}Si MAS-NMR spectra, extended on an unusually large field of chemical shift [39, 59]. ^{29}Si MAS-NMR spectra of MCM-22(P) have been observed and slightly differ according to composition and methods of synthesis [39, 69, 70].

The ^{29}Si MAS-NMR spectrum of sample MWW(P) (Figure 5a) was in good agreement with literature spectra of (MCM-22(P) samples with similar Si/Al ratio [69]. Chemical

shift and relative intensity of the deconvolution components are given in the supplementary materials in Table S1. Sample MWW(P) presented Q3 Si(1OH) signals between -94 and -101 ppm, corresponding to 15.3 % of the Si signals. Fairly isolated peaks of T2 and T3 tetrahedra, exposed to the interlayer space (see Figure 2 for the T site nomenclature), were observed at, respectively, -104.5 and -110 ppm. A broad signal between -113 and -120 ppm corresponded to the Si(0Al) contributions of T6, T7 and T8 tetrahedra, lining the intralayer porosity.

The ^{29}Si MAS-NMR spectrum of sample pH1 (Figure 5b), when compared with the MWW(P) spectrum, presented a more defined peak at -113 ppm. The superposition of the spectrum components increased, due to a general line broadening, the average half-height linewidth moving from 240 to 320 Hz for, respectively, MWW(P) and pH1 samples. The peak at -113 ppm was formed by the converging shifts of several components: the upfield-shifted T6, T7 and T8 signals and the nearly 1 ppm downfield-shifted T1, T4 and T5 signals. Quite importantly, the fraction of Q3 Si(1OH) signals in sample pH1 was 14.8 %, nearly the same value as for sample MWW(P), suggesting that no significant condensation between layers has taken place, despite the shrinkage of the interlayer spacing.

3.2. Diluted acid treatments in the presence of Cu^{2+}

The nitric acid solutions used in the treatments represent an oxidizing environment. In the hypothesis that a transition metal catalyst could induce an oxidative degradation of HMI and make its extraction easier, we introduced Cu^{2+} cations in the diluted-acid treatment. Cu^{2+} was already used in dioxane acid solutions as a catalyst of hydrolysis of

Schiff bases, a reaction implying secondary amine intermediates [71]. The XRD patterns of MCM-22(P) treated by 20 % dioxane nitric acid solutions at pH 4 and different concentrations of Cu^{2+} are shown in Figure 6. The corresponding *c* cell parameters are reported in Table 1. A 0.2 mM concentration of Cu^{2+} brought no significant changes of the diffraction pattern of MWW(P) sample and the CupH4E-4 sample was equivalent to the pH4 sample, treated in the absence of copper cations. Treatments in the presence of higher concentration of Cu^{2+} induced a decrease of the *c* cell parameter (Table 1). Sample CupH4E-2, treated by a 0.02 M Cu^{2+} solution, presented a *c* value of 25.41 Å. The SDA content was 8.1 HMI p.u.c., indicating that the treatment with Cu^{2+} has extracted 22 % of the HMI of the MCM-22(P) MWW(P) sample, to be compared with 5 % extraction of HMI by the acid treatment in the absence of Cu^{2+} (see Table 1). A catalytic effect of Cu^{2+} on the degradation of HMI has probably contributed to the result.

The residual content of copper in CupH4E-2 was 0.38 Cu/Al (atomic ratio). Albeit no copper oxide phase was detectable by XRD, the copper present was an effective oxidation catalyst, as highlighted by the degradation of the SDA in thermal gravimetry (TG) tests in air flow. The TG curves of several samples are reported in Figure 7. As already reported in literature, a first mass loss due to water desorption was observed up to nearly 100 °C. Degradation of the SDA began around 200 °C and was usually completed around 700 °C. The TG curve of the CupH4E-2 sample followed a trend similar to the MWW(P) sample until a sudden mass loss centered around 475 °C completed the SDA degradation (Figure 7e). Nitrogen-bearing SDA are usually decomposed in several steps [72]. The first one, up to about 400 °C, corresponds to the release of light amines issued from the decomposition. This leaves carbonaceous

residues which are burned in several steps between 400 and 700 °C. It seems likely that the presence of copper species catalysed the combustion of carbonaceous HMI residues at a temperature much lower than in Cu-free samples.

The ^{29}Si MAS-NMR spectrum of sample CupH4-E2 (Figure 5c) was extremely similar to the one of sample pH1, suggesting that the extraction of nearly half the interlayer SDA brought to a structure deformation of MCM-22(P) analogous to the extraction of a double amount of HMI. The average half-height linewidth was 322 Hz and the fraction of Q3 Si(1OH) signals was 14.2 %, values nearly identical to the ones of the pH1 sample.

3.3. Concentrated acid treatment

Treatment of MWW(P) by 70 % nitric acid led to significant dealumination, with the extraction of nearly 40 % of the initial aluminium (Table 1). The acid-treated AA sample retained an *a* value of 14.16 Å but presented a *c* parameter decreased from 26.8 to 25.1 Å (Table 1). As a consequence, the 002 peak moved from 6.59 to 7.07 °2Θ and was largely superposed to the 100 peak at 7.19 °2Θ, leading to a typical MWW diffraction pattern (Figure 8). Calcination of the AA sample completely eliminated the SDA, but induced a minimal evolution of the cell parameters.

The treatment by concentrated nitric acid removed nearly 60 % of the SDA (Table 1). It would be tempting to assume that the removed fraction of organics corresponds to easily extractable HMI in the interlayer space. An indirect confirmation of this assumption came from the comparison of these results with the effects of a similar treatment on a different zeolite. Treatment by 12 M HNO_3 on zeolite beta led to the

extraction of most the TEA template and to nearly complete dealumination [47]. Zeolite beta features a 3D network of 6.7 Å 12MR pores, large enough to allow easy extraction of TEA, unless it is retained by strong electrostatic forces [50]. The close charge-neutralisation relationship between the SDA cations and the anions of the aluminosilicate network implies that extraction of SDA and dealumination proceed as a concerted process. In the case of MCM-22(P), the extraction of HMI was easier from the 5.7 Å interlayer space than from the 4.0 Å 10MR intralayer pores. The retention of SDA in the intralayer pores would prevent the dealumination of a corresponding fraction of tetrahedra.

The ^{29}Si MAS-NMR spectra of MWW(P)C, AA and AAC samples are reported in Figure 9. The ^{29}Si MAS-NMR spectrum of MWW(P)C (Figure 9a) was in good agreement with literature spectra of MWW of corresponding aluminium content [73]. No significant Q3 peaks were observed, as expected in the case of a completely connected zeolite framework. Another significant variation by comparison with the MWW(P) spectrum was the important upfield shifts of signals of T7 and T8 tetrahedra, exposed to the intralayer porosity. This shift isolated the peak at -119.2 ppm, corresponding to the T6 signal, and contributed by shoulders to the main peak at -111 ppm.

The spectrum of the AA sample, treated with concentrated acid (Figure 9b) was fitted by taking into account the lower intensity of the Si(1Al) peaks due to dealumination. It showed a similar pattern to MWW(P)C with broader, more overlapping peaks. The average half-height width of the Q4 peaks was 240 Hz for MWW(P)C and 355 Hz for AA. Two Q3 peaks at -100.9 and 96.5 ppm accounted for 4.8% of the Si signal. It has been observed that the extraction of aluminium atoms from zeolite networks can give

rise to so-called hydroxyl nests, *i.e.* groups of four silanol groups, strongly hydrogen-bonded due to their converging orientation around the vacancy opened by aluminium extraction [74, 75]. As the level of dealumination of the AA sample corresponded to the extraction of nearly 1 % of the network tetrahedra, the formation of hydroxyl nests could account for most of the Q3 signal. In this case, the AA sample would feature completely connected layers with local vacancies due to dealumination. It can be also observed that the chemical shifts of the Q3 peaks suggest their attribution to T2 and T3 tetrahedra, exposed to the interlayer porosity, hence more easily dealuminated by combined acid-leaching of cationic SDA and anion-generating lattice aluminium.

Calcination of AA at 550 °C brought to the virtual elimination of the Q3 signals (Figure 9c). This can be coherent with the reported condensation of silanol nests by silicon migration in high-temperature treatments [76, 77]. Otherwise, the spectrum of AAC sample was similar to the AA's one, with marginally narrower peaks (average half-height width 337 Hz).

4. Conclusions

The 2D-3D transition in the calcination of the layered MCM-22(P) precursor to the 3D MCM-22 zeolite corresponds to a decrease of the *c* cell parameter from 26.4 to 25 Å. A similar reduction of *c* cell size obtained by template extraction in milder conditions has often been considered as an evidence of condensation of the precursor layers to a 3D structure without the need of a thermal treatment.

In this work, we have shown that a combined organic solvent-acid treatment in mild conditions removes organic template from the interlayer space of MCM-22(P), with a

decrease of the *c* cell parameter to 25 Å. The addition of copper ion catalysts enhanced the extraction of the SDA in still milder conditions. However, ^{29}Si MAS-NMR data indicated that no condensation of the interlayer silanols had taken place and no 3D structure had been formed by acid treatment at pH 1, despite the observed shrinkage of the interlayer space.

Reflux treatment by 70 % nitric acid provided complete extraction of SDA from the interlayer space with the same reduction in the *c* cell parameter to 25 Å. In this case, ^{29}Si MAS-NMR showed the formation of a partially dealuminated 3D zeolite structure. The dehydrating properties of the concentrated acid allowed the dehydration-condensation of silanols between opposite layers of the precursor, similarly to the results obtained by calcination.

Beyond the specific example of the condensation of the MWW precursor, chemical methods of condensation seem promising for the current developments in the elaboration of new zeolite networks by aggregation of layered precursors [2-4].

References

[1] A. Corma, V. Fornes, J. Martinez-Triguero, S. B. Pergher, J. Catal. 186 (1999) 57-63. https://doi.org/10.1006/jcat.1999.2503

[2] W. J. Roth, P. Nachtigall, R. E. Morris, P. S. Wheatley, V. R. Seymour, S. E. Ashbrook, P. Chlubná, L. Grajciar, M. Položij, A. Zukal, O. Shvets, J. Čejka, Nat. Chem. 5 (2013) 628–633. https://doi.org /10.1038/NCHEM.16

[3] W. J. Roth, P. Nachtigall, R. E. Morris, J. Čejka, Chem. Rev. 114 (2014) 4807–4837. https://doi.org /10.1021/cr400600f

[4] M. Mazur, P. S. Wheatley, M. Navarro, W. J. Roth, M. Položij, A. Mayoral, P. Eliášová, P. Nachtigall, J.Čejka, R. E. Morris, Nat. Chem. 2016, 8, 58-62. https://doi.org/10.1038/NCHEM.2374

[5] B. Marler, H. Gies, Eur. J. Mineral. 24 (2012) 405–428. https://doi.org /10.1127/0935-1221/2012/0024-2187

[6] F. S. O. Ramos, M. K. de Pietre, H. O. Pastore, RSC Adv. 3 (2013) 2084-2111 https://doi.org/10.1039/c2ra21573j

[7] J. Přech, P. Pizarro, D. P. Serrano, J. Cejka, Chem. Soc. Rev. 47 (2018) 8263-8306 https://doi.org/10.1039/c8cs00370j

[8] E. Schulman, W. Wu, D. Liu, Materials 13 (2020) 1822. https://doi.org /10.3390/ma13081822

[9] M. Shamzhy, B. Gil, M. Opanasenko, W. J. Roth, J. Čejka, ACS Catal. 11 (2021) 2366-2396. https://doi.org /10.1021/acscatal.0c05332

[10] A. J. Blake, K. R. Franklin, B. M. Lowe, J. Chem. Soc. Dalton Trans. 1988, 2513-2517. https://doi.org /10.1039/DT9880002513

[11] L. Schreyeck, P. Caullet, J. C. Mougenel, J. L. Guth, B. Marler, Microp. Mater. 6 (1996) 259-271. https://doi.org/10.1016/0927-6513(96)00032-6

[12] S. Zanardi, A. Alberti, G. Cruciani, A. Corma, V. Fornes, M. Brunelli, Angew. Chem. 116 (2004) 5041-5045. https://doi.org /10.1002/anie.200460085

[13] T. Ikeda, Y. Akiyama, Y. Oumi, A. Kawai, F. Mizukami, Angew. Chem. Int. Ed. 43 (2004) 4892-4896. https://doi.org /10.1002/anie.200460168

[14] B. Marler, N. Ströter, H. Gies, Micropor. Mesopor. Mat. 83 (2005) 201-211. https://doi.org/10.1016/j.micromeso.2005.04.007

[15] Y. X. Wang, H. Gies, J. H. Lin, Chem. Mater. 19 (2007) 4181-4188. https://doi.org/10.1021/cm0706907

[16] T. Moteki, W. Chaikittisilp, A. Shimojima, T. Okubo, J. Am. Chem. Soc. 130 (2008) 15780–15781. https://doi.org/10.1021/ja806930h

[17] A. Rojas, M. A. Camblor, Chem. Mater. 2014, 26, 1161-1169. https://doi.org/10.1021/cm403527t

[18] K. Varoon, X. Zhang, B. Elyassi, D. D. Brewer, M. Gettel, S. Kumar, A. Lee, S. Maheshwari, A. Mittal, C.-Y. Sung, M. Cococcioni, L. F. Francis, A. V. McCormick, K. A. Mkhoyan, M. Tsapatsis, Science 2011, 334, 72-75. https://doi.org/10.1126/science.1208891

[19] R. E. Morris, J. Cejka, Nat. Chem. 7 (2015) 381-388. https://doi.org/10.1038/NCHEM.2222

[20] W. J. Roth, T. Sasaki, K. Wolski, Y. Song, D.-M- Tang, Y. Ebina, R. Ma, J. Grzybek, K. Kałahurska, B. Gil, M. Mazur, S. Zapotoczny1, J. Cejka, Sci. Adv. 6 (2020) eaay8163. https://doi.org/10.1126/sciadv.aay816

[21] W. J. Roth, T. Sasaki, K. Wolski, Y. Ebina, D.-M. Tang, Y.i Michiue, N. Sakai, R. Ma, O. Cretu, J. Kikkawa, K. Kimoto, K. Kalahurska, B. Gil, M. Mazur, S. Zapotoczny, J. Čejka, J. Grzybek, A. Kowalczyk, J. Am. Chem. Soc. 143 (2021) 11052−11062. https://doi.org/10.1021/jacs.1c04081

[22] P. Eliašova, M. Opanasenko, P. S. Wheatley, M. Shamzhy M. Mazur, P. Nachtigall, W. J. Roth, R. E. Morris, J. Čejka, Chem. Soc. Rev. 44 (2015) 7177-7206. https://doi.org/10.1039/c5cs00045a

[23] M. V. Opanasenko, W. J. Roth, J. Čejka, Catal. Sci. Technol. 6 (2016) 2467–2484. https://doi.org/10.1039/c5cy02079d

[24] C. Perego, P. Ingallina, Catal. Today 73 (2003) 3–22. https://doi.org/10.1016/S0920-5861(01)00511-9

[25] G. C. Laredo, R. Quintana-Solórzano, J. J. Castillo, H. Armendáriz-Herrera, J. L. Garcia-Gutierrez, Appl. Catal. A: Gen. 454 (2013) 37-45. https://doi.org/10.1016/j.apcata.2013.01.001

[26] C. Perego, A. de Angelis, P. Pollesel, R. Millini, Ind. Eng. Chem. Res. 60 (2021) 6379−6402. https://doi.org/10.1021/acs.iecr.0c05886

[27] M. E. Leonowicz, J. A. Lawton, S. L. Lawton, M. K. Rubin, Science 264 (1994) 1910-1913. https://doi.org/10.1126/science.264.5167.1910

[28] G. Bellussi, G. Perego, M.G. Clerici, A. Giusti, EP 0293032 (2008)

[29] S. I. Zones, D. I. Holtermann, R. A. Innes, T. A. Pecoraro, D. S. Santilli, J. N. Ziemer. U.S. Pat. 4,826,667 (1989)

[30] M. J. Diaz Cabañas, M. A. Fernandez Camblor, C. Corell Martires, A. Corma Canos, EP 0818417 A1 (1997)

[31] C. T. Kresge, W. J. Roth, K. J. Simmons, J. C. Vartuli, U.S. 5,229,341 (1993)

[32] R. Millini, G. Perego, W. O. Parker, G. Bellussi, L. Carluccio, Microp. Mater. 4 (1995) 221-230. https://doi.org/10.1016/0927-6513(95)00013-Y

[33] W. Schwieger, G. Lagaly, in: S.M. Auerbach, K.A. Carrado, P.K. Dutta (Eds.). Handbook of Layered Materials, Marcel Dekker, New York, 2004, pp. 541-629.

[34] S. B. C. Pergher, A. Corma, V. Fornes, Quim. Nova, 26 (2003) 795-802. https:/doi.org/10.1590/S0100-40422003000600003

[35] https://europe.iza-structure.org/databases/ModelBuilding/MWW.pdf (accessed 30 november 2021)

[36] L. Puppe, J. Weiser, U.S. Pat. 4,439,409 (1984)

[37] M. K. Rubin, P. Chu, U.S. Pat. 4,954,325 (1990)

[38] C. D. Chang, D. M. Mitko, U.S. Pat. 5,173,281 (1992)

[39] M. A. Camblor, C. Corell, A. Corma, M.-J. Diaz-Cabañas, S. Nicolopoulos, J.M. Gonzalez-Calbet, M. Vallet-Regı, Chem. Mater. 8 (1996) 2415-2417. https://doi.org/10.1021/cm960322v

[40] S. L. Lawton, A. S. Fung, G. J. Kennedy, L. B. Alemany, C. D. Chang, G. H. Hatzikos, D. N. Lissy, M. K. Rubin, H.-K. C. Timken, S. Steuernagel, D. E. Woessner, J. Phys. Chem. 100 (1996) 3788-3798. https://doi.org/10.1021/jp952871e

[41] D. Vuono, L. Pasqua, F. Testa, R. Aiello, A. Fonseca, T.I. Korányi, J. B.Nagy, in: E. van Steen, I.M. Claeys, L.H. Callanan (Eds.), Recent Advances in the Science and Technology of Zeolites and Related Materials. Stud. Surface Sci. Catal. 154, Part A, Elsevier, Amsterdam, 2004, pp. 203-210. https://doi.org/10.1016/S0167-2991(04)80803-6

[42] W. J. Roth, J. Čejka, Catal. Sci. Technol., 1 (2011) 43–53. https://doi.org/10.1039/c0cy00027b

[43] W. J. Roth, D. L. Dorset, Micropor. Mesopor. Mat. 142 (2011) 32-36. https://doi.org/10.1016/j.micromeso.2010.11.007

[44] J. Grzybek, W. J. Roth, B. Gil, A. Korzeniowska, M. Mazur, J. Čejka, R. E. Morris, J. Mater. Chem. A, 7 (2019) 7701–7709. https://doi.org/10.1039/c8ta09826c

[45] X. Meng, F.-S. Xiao, Chem. Rev. 114 (2014) 1521-1543. https://doi.org/10.1021/cr4001513

[46] T. Pan, Z. Wu, A.C.K. Yip, Catalysts 9 (2019) 274. https://doi.org/10.3390/catal9030274

[47] E. Bourgeat-Lami, F. Fajula, D. Anglerot, T. Des Courières, Microp. Mater. 1 (1993) 237-245. https://doi.org/10.1016/0927-6513(93)80067-5

[48] F. Di Renzo, S. Gomez, F. Fajula, R. Teissier, WO 9605060 (1996)

[49] F. Di Renzo, S. Gomez, R. Teissier, F. Fajula, in: A. Corma, F. V. Melo, S. Mendioroz, José L. G. Fierro (Eds.), 12th International Congress on Catalysis, Stud. Surface Sci. Catal. 130, Elsevier, Amsterdam, 2000, pp. 1631-1636. https://doi.org/10.1016/S0167-2991(00)80434-6

[50] C. W. Jones, K. Tsuji, T. Takewaki, L. W. Beck, M. E. Davis, Micropor. Mesopor. Mat. 48 (2001) 57-64. https://doi.org/10.1016/S1387-1811(01)00330-4

[51] L. Wang, Y. Wang, Y. Liu, L. Chen, S. Cheng, G. Gao, M. He, P. Wu, Micropor. Mesopor. Mat. 113 (2008) 435-444. DOI :10.1016/j.micromeso.2007.11.044

[52] M. Hu, B. Zhao, D.-Y. Zhao, M.-T. Yuan, H. Chen, Q.-Q. Hao, M. Sun, L. Xu, X. Ma, RSC Adv. 8 (2018) 15372-15379. https://doi.org/10.1039/c8ra00212f

[53] E. Verheyen, L. Joos, K. Van Havenbergh, E. Breynaert, N. Kasian, E. Gobechiya, K. Houthoofd, C. Martineau, M. Hinterstein, F. Taulelle, V. Van Speybroeck, M. Waroquier, S. Bals, G. Van Tendeloo, C. E. A. Kirschhock, J. A. Martens, Nat. Mater. 11 (2012) 1059-1064. https://doi.org/10.1038/NMAT3455

[54] P. Wheatley, P. Chlubna-Eliasova, H. Greer, W. Zhou, V. R. Seymour, D. M. Dawson, S. E. Ashbrook, A. B. Pinar, L. B. McCusker, M. Opanasenko, J. Cejka, R. E. Morris, Angew. Chem. Int. Ed. 53 (2014) 13210–13214. https://doi.org/10.1002/anie.201407676

[55] D. S. Firth, S. A. Morris, P. S. Wheatley, S. E. Russell, A. M. Z. Slawin, D. M. Dawson, A. Mayoral, M. Opanasenko, M. Polozij, J. Cejka, P. Nachtigall, R. E. Morris, Chem. Mater. 29 (2017) 5605–5611. https://doi.org/10.1021/acs.chemmater.7b01181

[56] M. Mazur, A. Arevalo-Lopez, P. S. Wheatley, G. P. M. Bignami, S. E. Ashbrook, A. Morales-Garcia, P. Nachtigall, J. P. Attfield, J. Cejka, R. E. Morris, J. Mater. Chem. A, 6 (2018) 5255–5259. https://doi.org/10.1039/c7ta09248b

[57] I. C. Medeiros-Costa, E. Dib, N. Nesterenko, J.-P. Dath, J.-P- Gilson, S. Mintova, Chem. Soc. Rev. 50 (2021) 11156-11179. https://doi.org/10.1039/d1cs00395j

[58] S. Unverricht, M. Hunger, S. Ernst, H.G. Karge, J. Weitkamp, in: J. Weitkamp, H.G. Karge, H. Pfeifer, W. Hölderich (Eds.), Zeolites and Related Microporous Materials: State of the Art 1994, Studies in Surface Science and Catalysis 84, Elsevier 1994, pp. 37-44.

[59] M. A. Camblor, A. Corma, M.-J. Dıaz-Cabañas, J. Phys. Chem. B 102 (1998) 44-51. https://doi.org/10.1021/jp972319k

[60] G. J. Kennedy, S. L. Lawton, M. K. Rubin, J. Am. Chem. Soc. 116 (1994) 11000-11003. https://doi.org/10.1021/ja00103a015

[61] G. J. Kennedy, S. L. Lawton, A. S. Fung, M.K. Rubin, S. Steuernagel, Catalysis Today 49 (1999) 385-399. https://doi.org/10.1016/S0920-5861(98)00444-1

[62] G. Engelhardt, U. Lohse, V. Patzelova, M. Mägi, E. Lippmaa, Zeolites 3 (1983) 233-238. https://doi.org/10.1016/0144-2449(83)90013-1

[63] W. Lutz, D. Täschner, R. Kurzhals, D. Heidemann, C. Hübert, Z. Anorg. Allg. Chem. 635 (2009) 2191–2196. https://doi.org/10.1002/zaac.200900237

[64] Y. Oumi, T. Takeoka, T. Ikeda, T. Yokoyama, T. Sano, New J. Chem. 31 (2007) 593–597. https://doi.org/10.1039/b617361f

[65] P. Wu, T. Komatsu, T. Yashima, Micropor. Mesopor. Mat. 22 (1998) 343-356. https://doi.org/10.1016/S1387-1811(98)00114-0

[66] J. Méring, Acta Cryst. 2 (1949) 371-377. https://doi.org/10.1107/S0365110X49000977

[67] D. M. Moore, R.C. Reynolds, X-Ray Diffraction and the Identification and Analysis of Clay Minerals, Oxford University Press, Oxford, 1989, pp. 241-271.

[68] S. Guggenheim, in: M.F. Brigatti, A. Mottana (Eds,), Layered Mineral Structures and their Application in Advanced Technologies. European Mineralogical Union Notes in Mineralogy 11, 2011, pp. 73-121. https://doi.org/10.1180/EMU-notes.11.2

[69] W. Kolodziejski, C. Zicovich-Wilson, C. Corell, J. Pérez-Pariente, A. Corma, J. Phys. Chem. 99 (1995) 7002-7008. https://doi.org/10.1021/j100018a037

[70] W. J. Roth, D. L. Dorset, G. J. Kennedy, Micropor. Mesopor. Mat. 142 (2011) 168–177. https://doi.org/10.1016/j.micromeso.2010.10.052

[71] M. A. El-Taher, J. Chin. Chem. Soc.-Taip. 45 (1998) 815-820. https://doi.org/10.1002/jccs.199800123

[72] E. Bourgeat-Lami, F. Di Renzo, F. Fajula, P. H. Mutin, T. Des Courières, J. Phys. Chem. 96 (1992) 3807-3811. https://doi.org/10.1021/j100188a044

[73] B. Gil, B. Marszałek, A. Micek-Ilnicka, Z. Olejniczak, Top. Catal. 53 (2010) 1340–1348. https://doi.org/10.1007/s11244-010-9592-7

[74] J. Lynch, F. Raatz, P. Dufresne, Zeolites 7 (1987) 333-340. https://doi.org/10.1016/0144-2449(87)90036-4

[75] W. Lutz, Adv. Mater. Sci. Eng. 2014, 724248. https://doi.org/10.1155/2014/724248

[76] T. Kawai, K. Tsutsumi, J. Colloid Interf. Sci. 213 (1999) 310–316. https://doi.org/10.1006/jcis.1999.6093

[77] W. Lutz, R. A. Shutilov, V. Y. Gavrilov, Z. Anorg. Allg. Chem. 640 (2014) 577–581. https://doi.org/10.1002/zaac.201300403

Table 1. Composition and cell parameters of samples. Effects of calcination and acid treatments.

	Si/Al	HMI/ cell	P6/mmm cell	
			a / Å	c / Å
MWW(P)	23	10.3	14.16(1)	26.81(1)
pH4	23	9.8	14.16(0)	26.78(1)
pH3	23	10.0	14.16(2)	26.38(2)
pH2	23	8.1	14.15(4)	25.72(2)
pH1	25	6	14.15(1)	25.05(4)
pH1C	25	0	14.15(2)	25.21(3)
CupH4E-4	23	n.a.	14.15(4)	26.81(1)
CupH4E-3	23	n.a.	14.15(1)	26.65(1)
CupH4E-2	23	n.a.	14.14(4)	25.40(6)
CupH4E-2C	23	0	14.16(3)	24.98(2)
AA	39	4.4	14.15(6)	25.11(1)
AAC	39	0	14.15(6)	25.30(4)
MWW(P)C	23	0	14.15(5)	25.26(4)

Figure captions.

Figure 1. Condensation of the layers of MCM-22(P) to form MCM-22 and nomenclature of the tetrahedra of the MWW structure. HMI is hexamethyleneimine. Modified from Pergher *et al*. [34] and from the IZA structure database [35].

Figure 2. Evolution of the XRD pattern of MCM-22(P) upon calcination, with decrease of the *c* cell parameter and formation of MCM-22.

Figure 3. Evolution of the XRD pattern of MWW(P) upon treatment by diluted HNO_3 in organic solvent and calcination: samples MWW(P) (a), pH4 (b), pH3 (c), pH2 (d), pH1 (e), pH1C (f), MWW(P)C (g).

Figure 4. Scanning electron micrograph of MWW(P)C sample.

Figure 5. ^{29}Si MAS-NMR spectra of samples MWW(P) (a), Ph1 (b) and CupH4 (c). For each sample, the top trace is the experimental spectrum, the mid trace is the simulated one, and the lower traces are the components of the deconvolution.

Figure 6. Evolution of the XRD pattern of MWW(P) upon treatment by diluted HNO_3 in organic solvent in the presence of Cu^{2+} cations: samples MWW(P) (a), CupH4E-4 (b), CupH4E-3 (c), CupH4E-2 (d), CupH4E-2C (e), MWW(P)C (f).

Figure 7. TG curves of samples. MWW(P) (a), pH2 (b), AA (c), MWW(P)C (d), CupH4E-2 (e).

Figure 8. Evolution of the XRD pattern of MWW(P) upon calcination or treatment by concentrated HNO_3: samples MWW(P) (a), MWW(P)C (b), AA (c), AAC (d).

Figure 9. ^{29}Si MAS-NMR spectra of samples MWW(P)C (a), AA (b) and AAC (c). For each sample, the top trace is the experimental spectrum, the mid trace is the simulated one, and the lower traces are the components of the deconvolution.

Figure 1.

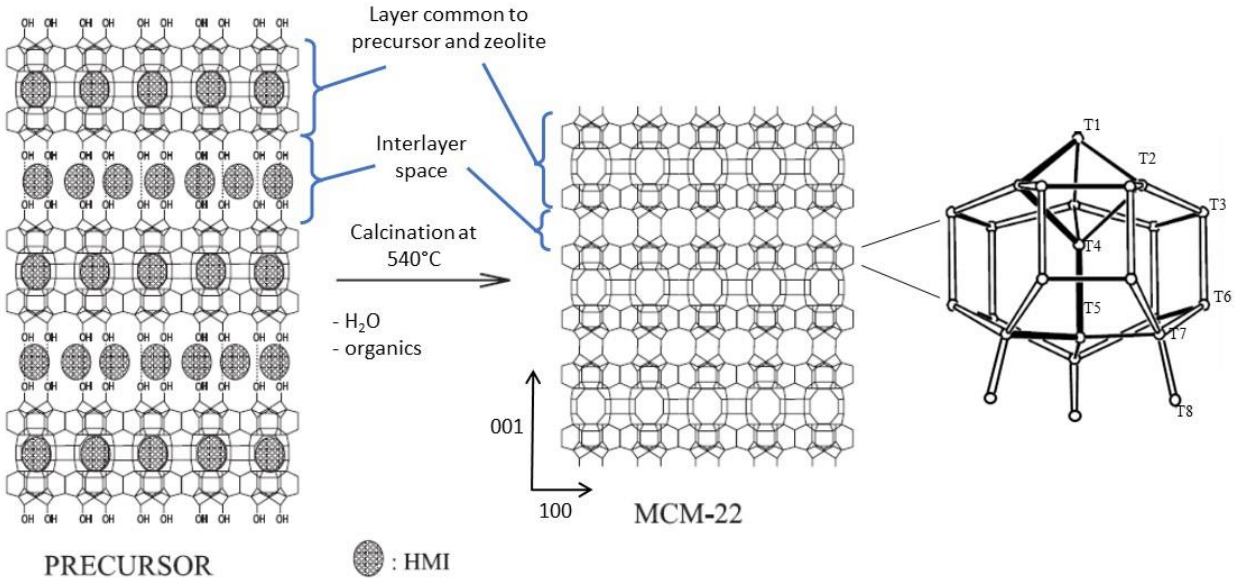

Figure 2.

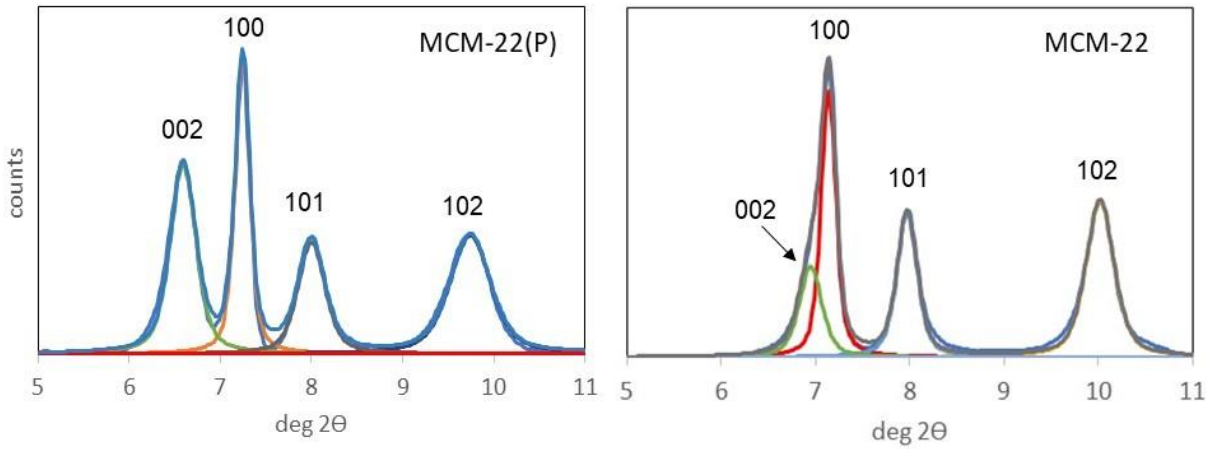

Figure 3.

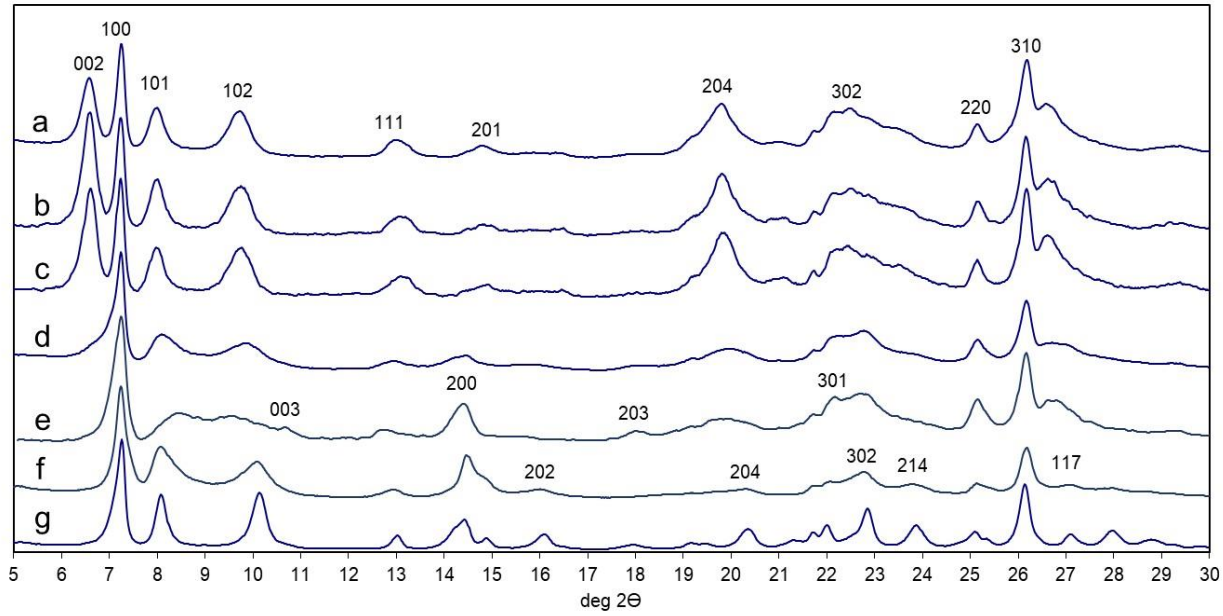

Figure 4.

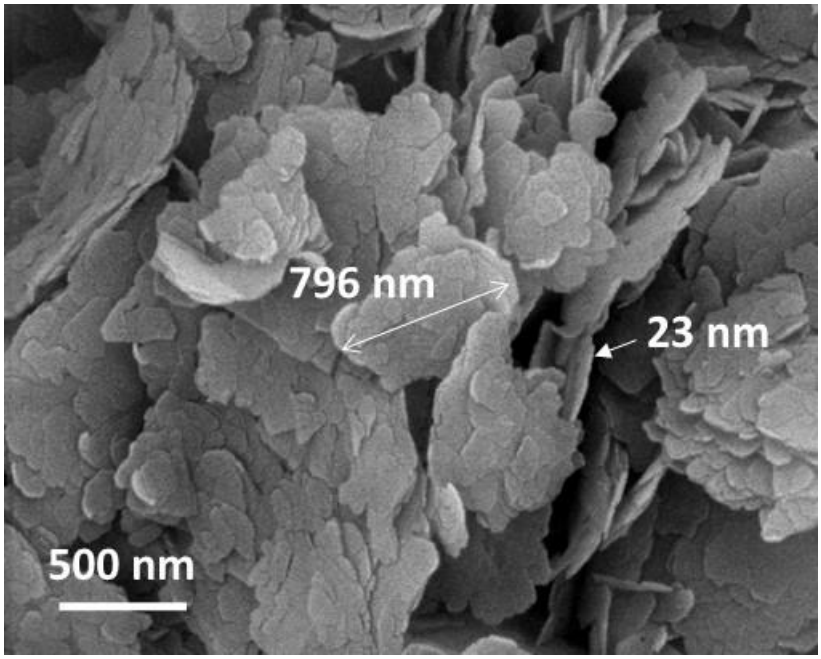

Figure 5.

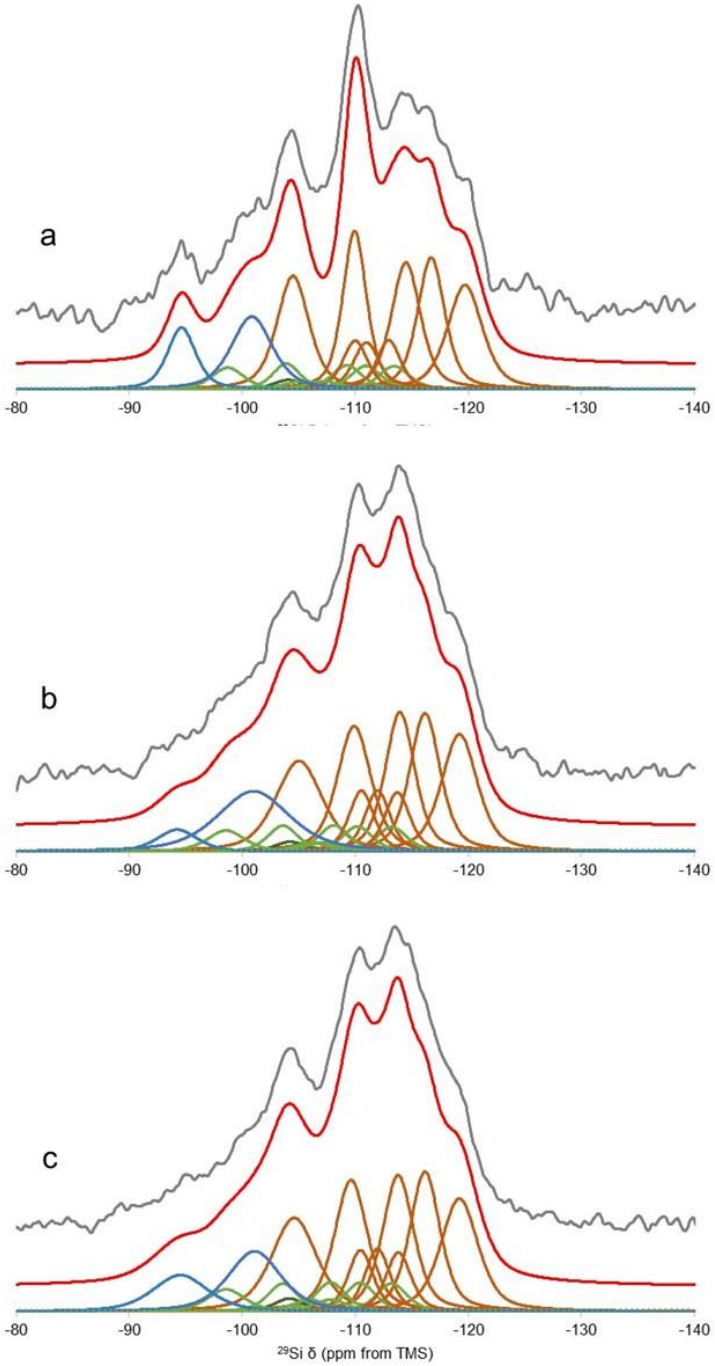

Figure 6.

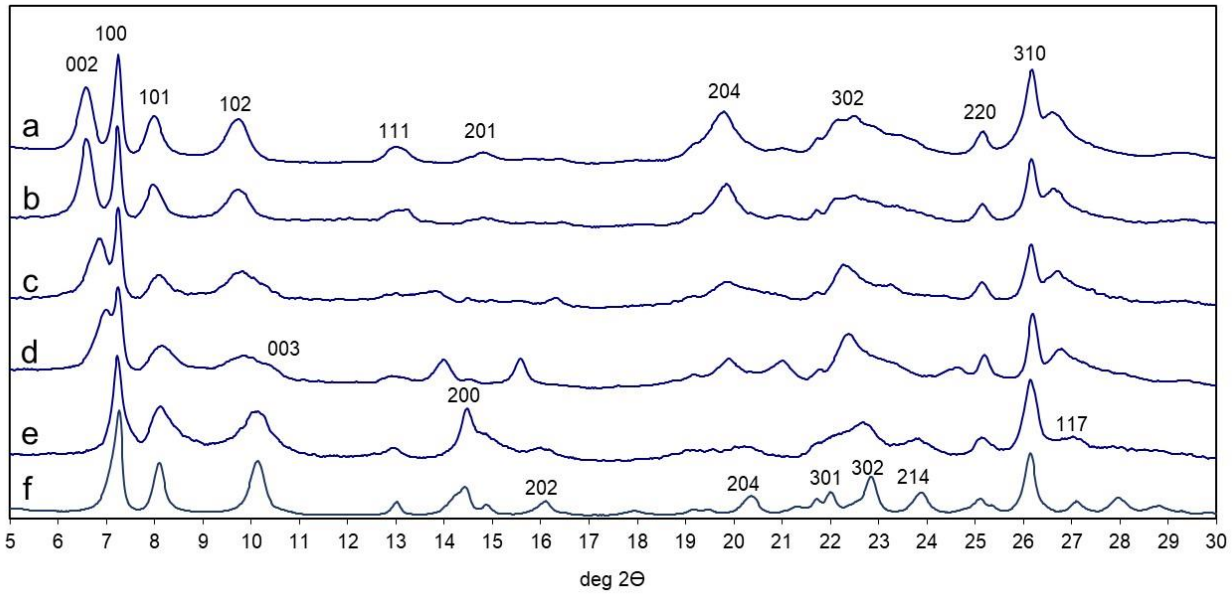
100
002
101
102
111
201
204
302
220
310
a
b
c
d
003
200
e
117
f
202
204
301
302
214
5 6 7 8 9 10 11 12 13 14 15 16 17 18 19 20 21 22 23 24 25 26 27 28 29 30
deg 2Θ

Figure 7.

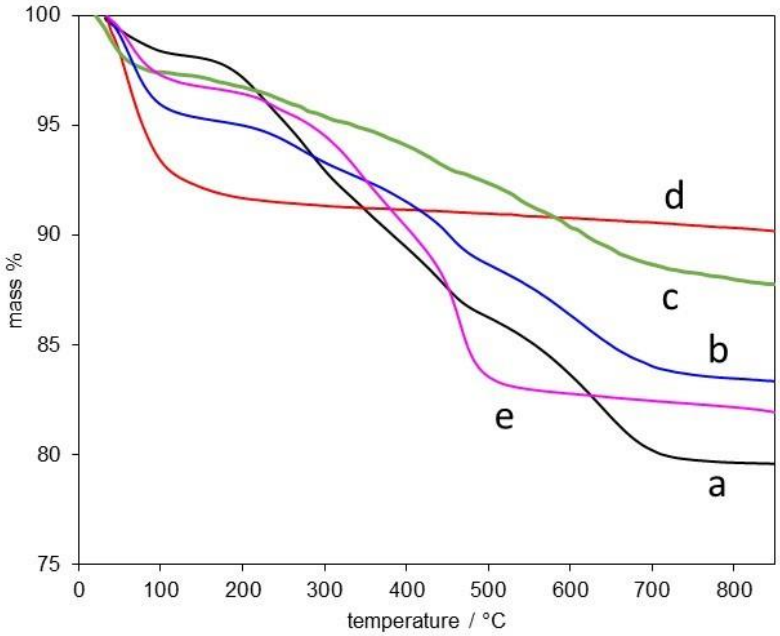

Figure 8.

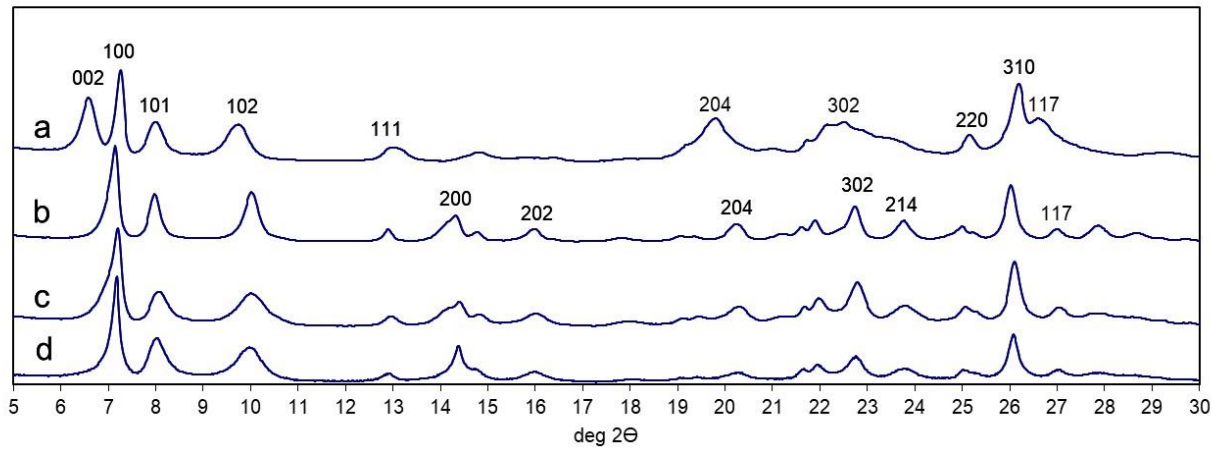

Figure 9.